LIGHTCURVES OF NINETEEN ASTEROIDS

Eric V. Dose
3167 San Mateo Blvd NE #329
Albuquerque, NM 87110
mp@ericdose.com

(Received: 2022 October 15 Revised: 2022 November 12)

We present lightcurves, synodic rotation periods, and G slope value (H-G) estimates for nineteen asteroids.

We present asteroid lightcurves obtained via the workflow process described by Dose (2020) and as later improved (Dose, 2021a). This workflow applies to each image an ensemble of typically 20-60 nearby comparison ("comp") stars selected from the ATLAS refcat2 catalog (Tonry et al., 2018). Custom diagnostic plots and the abundance of comp stars allow for rapid identification and removal of outlier, variable, and poorly measured comp stars.

The product of this custom workflow is one night's time series of absolute magnitudes for the target asteroid, all on Sloan r' (SR) catalog basis. These magnitudes are imported directly into *MPO Canopus* software (Warner, 2021) where they are adjusted for distances and phase-angle dependence, fit by Fourier analysis including identifying and ruling out of aliases, and plotted. Phase-angle dependence is corrected with a H-G model, using the G slope value minimizing best-fit RMS error across all nights' data. No nightly zero-point adjustments (DeltaComps in *MPO Canopus* terminology) were made to any session herein, other than by adjusting the G slope value (H-G phase model).

Lightcurve Results

Nineteen asteroids were observed from New Mexico Skies Observatory at 2310 meters elevation in southern New Mexico. Images were acquired with a 0.35 m SCT reduced to f/7.7; a SBIG STXL-6303E camera cooled to -35 C and fitted with an Exoplanet/Blue Blocker (BB) filter (Astrodon); and a PlaneWave L-500 mount. The equipment was operated remotely via ACP software (DC-3 Dreams, version 8.3), running plan files generated for each night by the author's python scripts (Dose, 2020). Exposures were autoguided, and exposure times targeted 3-4 millimagnitudes uncertainty in asteroid instrumental magnitude, subject to a minimum exposure of 150 seconds to ensure suitable comp-star photometry, and to a maximum of 900 seconds.

FITS images were plate-solved by *PinPoint* (DC-3 Dreams) or *TheSkyX* (Software Bisque) and were calibrated using temperature-matched, median-averaged dark images and recent flat images of a flux-adjustable flat panel. Every photometric image was visually inspected; the author excluded all images with poor tracking, obvious interference by cloud or moon, or having stars, satellite tracks, cosmic ray artifacts, or other apparent light sources within 10 arcseconds of the target asteroid. Images passing these screens were submitted to the workflow. The BB filter, a yellow filter with relatively sharp wavelength cut-off, requires only a modest first-order transform to the standard Sloan r' passband. Using this BB filter, rather than a clear filter or no filter, improves night-to-night reproducibility to a degree outweighing any loss of signal-to-noise ratio.

In this work, "period" refers to an asteroid's synodic rotation period, "SR" denotes the Sloan r' passband, and "mmag" denotes millimagnitudes (0.001 magnitude).

<u>282 Clorinde</u>. This inner main-belt asteroid has numerous published rotation periods (6.42 h, Binzel and Mulholland, 1983; 12.142 h, Behrend, 2018web; 49.365 h, Ďurech et al., 2020; 49.352 h, Bonamico and van Belle, 2021; and 49.350 h, Pilcher, 2022). We confirm the more recent reports with our determination of 49.280 ± 0.006 h. Our lightcurve is built from 12 nights' data taken over 12 weeks; a large number of nights is needed to obtain full coverage as the period is rather close to two sidereal days. The lightcurve shape is clearly bimodal. Our best estimate of G (H-G phase model) is 0.03; Fourier fit RMS error is 7 mmag.

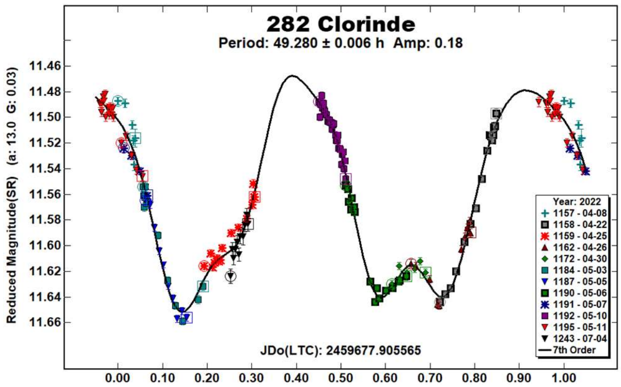

<u>414 Liriope</u>. For this outer main-belt asteroid, the author confirms the most recent period determinations (11.005 h, Colazo et al., 2020; 11.0065 h, Pál et al., 2020; 11.007 h, Dose, 2021c) with a new determination of 11.004 ± 0.001 h, derived from observations at a new viewing aspect (phase angle bisector). This new lightcurve (PAB = 209° longitude, 11° latitude) and the author's 2021 lightcurve (PAB = 147° longitude, 7° latitude) are remarkably similar in shape and amplitude, suggesting that 414 Liriope's rotational axis may be nearly aligned with the ecliptical axis. The present Fourier fit RMS error is 8 mmag; G value (H-G model) of roughly 0.16 gave optimum fit.

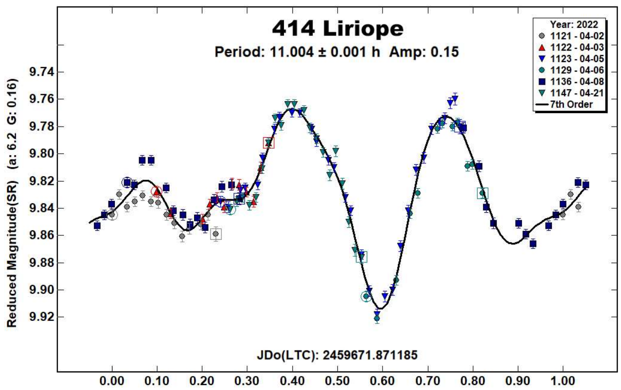

<u>866 Fatme</u>. New observations and period solution of 23.215 ± 0.001 h for this outer main-belt asteroid decidedly fail to confirm previous period reports, including the author's own from 2021 (20.03 h, Stephens, 2002; 9.4 h, Behrend, 2004web; 9.36 h, Behrend, 2012web; 20.7 h, Aznar Macias et al., 2016; 5.800 h, Polakis, 2018b; 11.600 h, Dose, 2021b). The new Fourier fit RMS error is 8 mmag, and best G value is approximately 0.08.

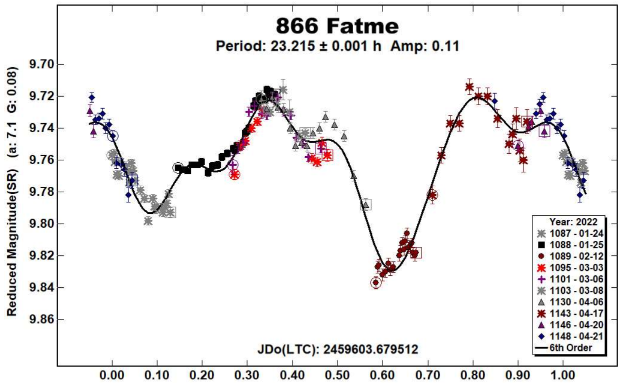

A split-halves plot of the new observations appears clearly support a bimodal interpretation. But the author's 2021 lightcurve at exactly half the present period appeared bimodal as well. And beyond that: Polakis' 2018 lightcurve with period 5.800 h, which is *one quarter* of the present solution, could itself be interpreted as bimodal. The author speculates that the asteroid's shape could be quite unusual but has no explanation for how these three relatively high-quality lightcurves could differ in such a manner. Most likely, this is a tale of caution where bi-modality assumptions fail for low amplitude objects (see Harris et al., 2014.).

866 Fatme clearly needs careful observation at future apparitions, and given the period's proximity to 24 (or 12) h, we recommend apparitions at very favorable latitude, in order to maximize session lengths. The next such apparitions are July 2024 for the Southern Hemisphere and March 2028 for the Northern Hemisphere.

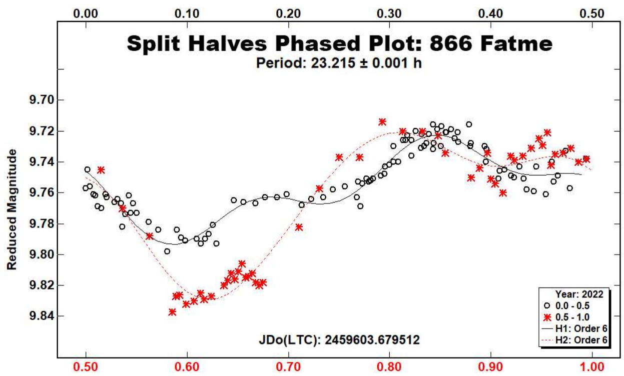

1051 Merope. We determine a synodic period of 13.710 ± 0.001 h for this Alauda-family, outer main-belt asteroid. Our result, built from 11 nights' data, agrees with that of Waszczak et al. (13.717 h, 2015) but differs from two other published solutions (27.2 h, Carbo et al., 2009; 6.85563 h, Pál et al., 2020). Our Fourier fit RMS error is 14 mmag; best G value was approximately -0.09. All positive values of G gave markedly worse fits.

The author notes that the 4 published periods show the same 1:2:4 pattern found for 866 Fatme mentioned above, though the 27.2 h lightcurve suffered incomplete phase coverage.

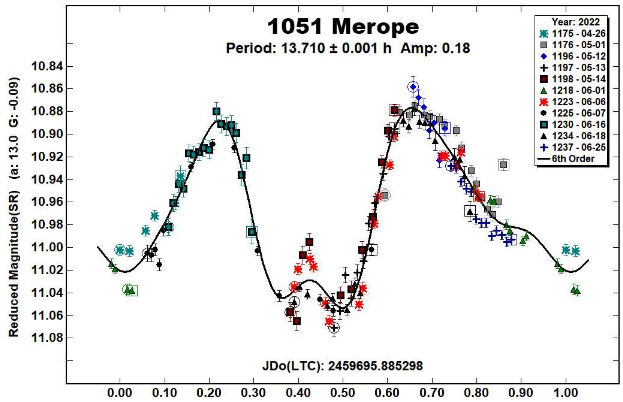

In our period spectrum, the 13.710 h solution dominates.

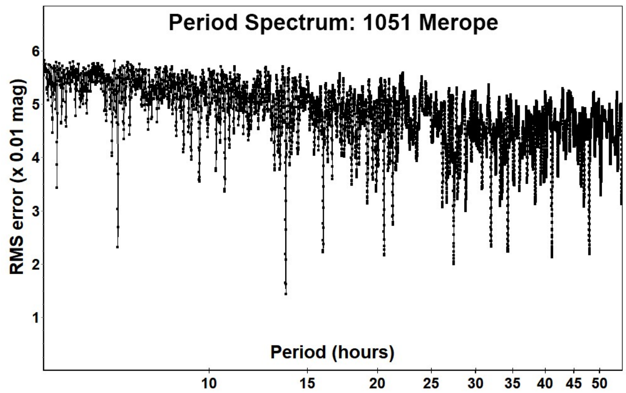

1237 Genevieve. This middle main-belt asteroid has had several reported rotation periods, all near 16.4 or 24.8 hours (16.37 h, Binzel, 1987; 24.82 h, Behrend, 2005web; 16.48 h, Polakis, 2018b; 24.6982 h, Ďurech et al., 2019; 16.31 h, Polakis, 2022). We report a period of 12.346 ± 0.004 h on a monomodal basis, which would give 24.692 h on a bimodal basis. Our lightcurve gave no indication of shape differences in alternating phases, nor does the amplitude of 0.21 magnitudes point clearly toward either basis, so the monomodal vs. bimodal nature of our lightcurve remains ambiguous. Our best G estimate is 0.15, the MPC nominal value, and Fourier RMS error is 9 mmag.

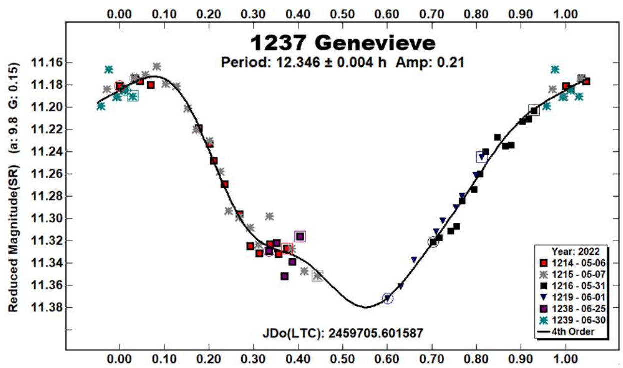

Our period spectrum disfavors rotation period estimates near 16 hours, which is an alias by ½ period per 24 hours of both period estimates 12 hours and 24 hours. This asteroid seems to call for a multi-longitude observation campaign, or a campaign benefiting from unusually favorable asteroid declination (and thus long observing sessions) to attempt to relieve the aliasing that apparently plagues single-location observation campaigns of 1237 Genevieve.

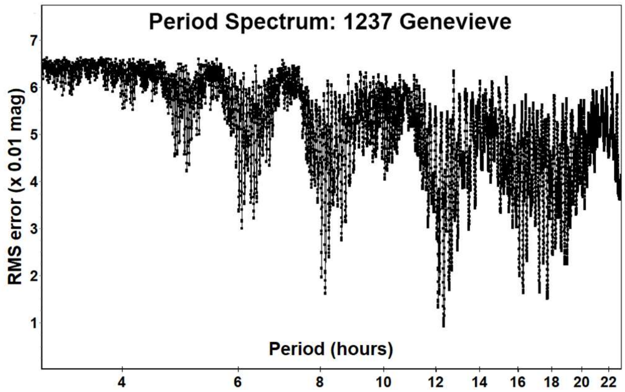

1255 Schilowa. This outer main-belt asteroid has had several rotation period reports in some disagreement (29.536 h, Behrend, 2005web; 29.7 h, Behrend, 2006web; > 24 h, Behrend, 2009web; 29.4674 h, Hanuš et al., 2013; 76.275 h, Polakis, 2018a; 38.4733 h, Pál et al., 2020). Our determination of 76.707 ± 0.019 h agrees approximately with that of Polakis and differs from the others. We note that Pál's period is half of ours, but that our lightcurve is clearly bimodal in shape. Our RMS error is 8 mmag, and our G value estimate is 0.02.

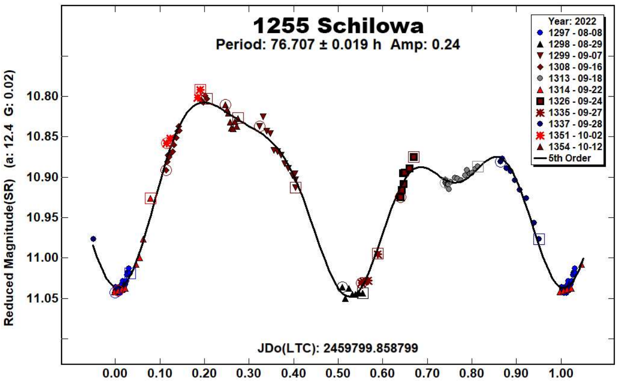

Previously reported periods near 29.6 h are an alias of our result by ½ period per sidereal day; the substantial number of our observing sessions has eliminated that alias from our period spectrum.

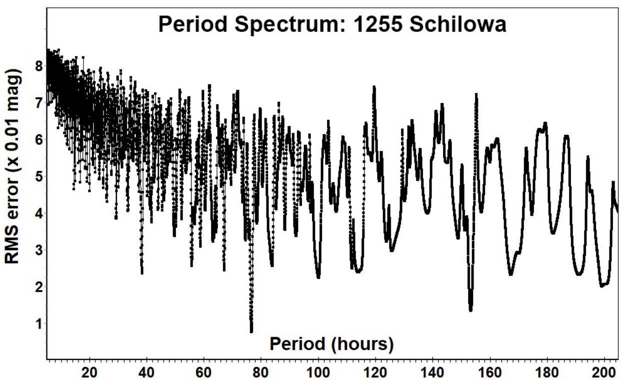

1261 Legia. For this outer main-belt asteroid, we find a period of 25.727 ± 0.002 h, differing from the sole known previous report of 8.693 h (Behrend, 2005web). Our RMS error is 16 mmag; G value of 0.07 minimized the fit error.

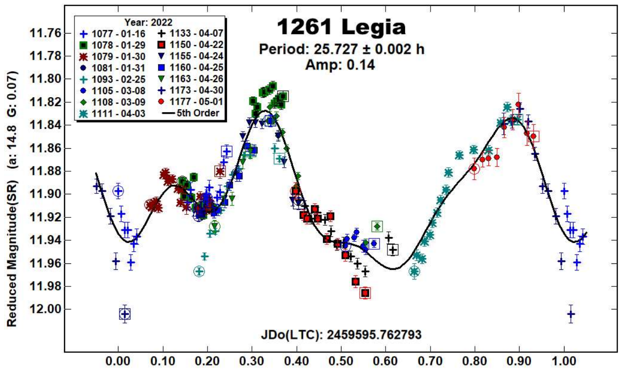

Our length of observation campaign (15 nights over 15 weeks) yields a period spectrum that supports our proposed period solution. The period spectrum does not support the previously reported period near 8.7 h.

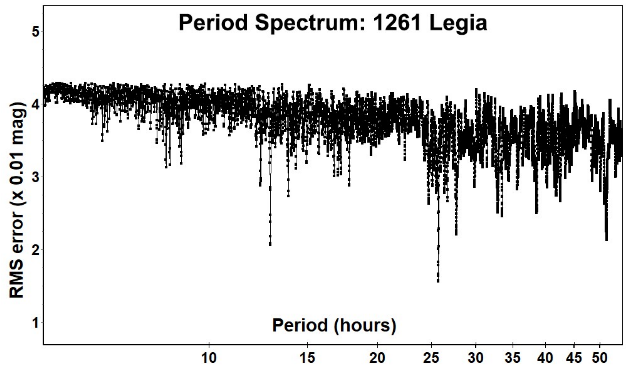

1300 Marcelle. Previous period reports (>12 h, Behrend, 2008 web; 17.9536 h, Pál et al., 2020) did not prepare us for the very long period estimate of 566.57±0.44 h that emerged from our 16 nights (across 14 weeks, about 3.8 period cycles) of observations of this outer main-belt asteroid. We have an unfortunate gap in observations around the major minimum (phase 0.93 in the lightcurve), but rest of the lightcurve is well covered, and the RMS error is only 17 mmag, or about 5% of the amplitude found. G value of 0.09 optimized the fit.

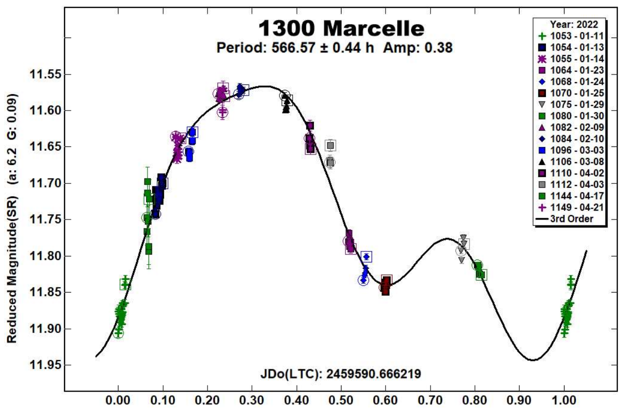

Number	Name	yyyy mm/dd	Phase	L_{PAB}	B_{PAB}	Period(h)	P.E.	Amp	A.E.	Grp
282	Clorinde	2022 04/08-07/04	*13.8,21.5	224	11	49.280	0.006	0.18	0.04	MB-I
414	Liriope	2022 04/02-04/21	*6.3,3.5	209	11	11.004	0.001	0.15	0.02	MB-O
866	Fatme	2022 01/24-04/21	*7.2,17.2	142	8	23.215	0.001	0.11	0.03	MB-O
1051	Merope	2022 04/26-06/25	*13.1,12.8	247	26	13.710	0.001	0.18	0.04	ALA
1237	Genevieve	2022 05/06-06/30	9.4,21.1	206	5	12.346	0.004	0.21	0.03	MB-M
1255	Schilowa	2022 06/08-10/12	*21.7,14.5	341	10	76.707	0.019	0.24	0.03	MB-O
1261	Legia	2022 01/16-05/01	*15.0,21.7	154	3	25.727	0.002	0.14	0.05	MB-O
1300	Marcelle	2022 01/11-04/21	*6.3,21.2	124	9	566.570	0.440	0.38	0.05	MB-O
1582	Martir	2022 03/08-04/29	*6.0,17.0	171	14	12.376	0.001	0.61	0.03	MB-O
1585	Union	2022 07/19-10/12	*11.0,21.1	320	4	12.800	0.001	0.22	0.04	MB-O
1605	Milankovitch	2022 09/24-10/04	10.2,6.8	24	-6	11.608	0.004	0.10	0.02	EOS
1724	Vladimir	2022 05/06-06/24	*10.9,11.7	248	15	12.569	0.002	0.26	0.04	MB-O
1904	Massevitch	2022 04/30-05/05	7.7,6.5	232	13	5.396	0.001	0.34	0.02	MB-O
2088	Sahlia	2022 04/02-05/02	11.0,22.3	174	0	59.550	0.008	0.90	0.03	FLO
2802	Weisell	2022 05/15-06/16	19.2,21.8	184	10	21.086	0.003	0.47	0.05	MB-O
3431	Nakano	2022 07/13-09/05	*15.0,4.4	332	4	9.056	0.002	0.13	0.03	MB-O
4429	Chinmoy	2022 09/05-10/14	*2.7,19.3	347	1	731.710	5.020	0.46	0.06	NYS
4901	O Briain	2022 07/27-09/06	*20.5,6.9	333	6	1.325	0.001	0.08	0.03	2076
12919	Tomjohnson	2022 07/18-09/24	*9.6,28.3	312	8	8.149	0.001	0.52	0.04	MB-I

Table I. Observing circumstances and results. The phase angle is given for the first and last date. If preceded by an asterisk, the phase angle reached an extrema during the period. L_{PAB} and B_{PAB} are the approximate phase angle bisector longitude/latitude at mid-date range (see Harris et al., 1984). Grp is the asteroid family/group (Warner et al., 2009).

Despite the gap in lightcurve phase coverage, our period spectrum appears to rule out periods shorter than about 300 h.

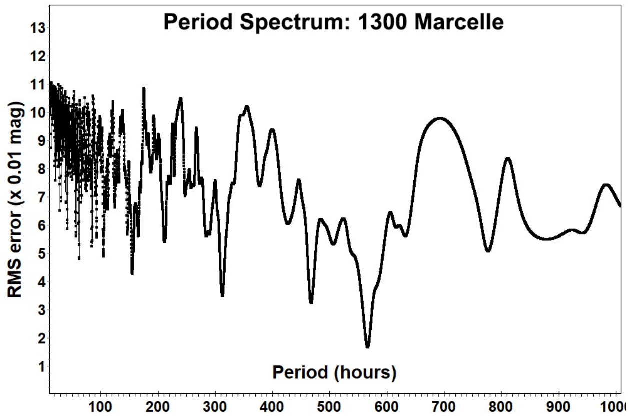

1582 Martir. This relatively well-studied outer main-belt asteroid has recently been found to have synodic rotation period near 12.37 h (12.37670 h, Ďurech et al., 2018; 12.366 h, McNeill et al., 2019; 12.3754 h, Pál et al., 2020; 12.372 h, Stephens and Warner, 2021); earlier reports differed (15.757 h, Warner, 2000; 15.668 h, Warner, 2006; 9.84 h, Warner, 2010). We were fortunate to observe 1582 Martir while its lightcurve amplitude was greater than previously reported, and we confirm the more recent reports with our period of 12.376 ± 0.001 h. Our Fourier fit RMS error is 16 mmag; G value of 0.04 minimized that fit error.

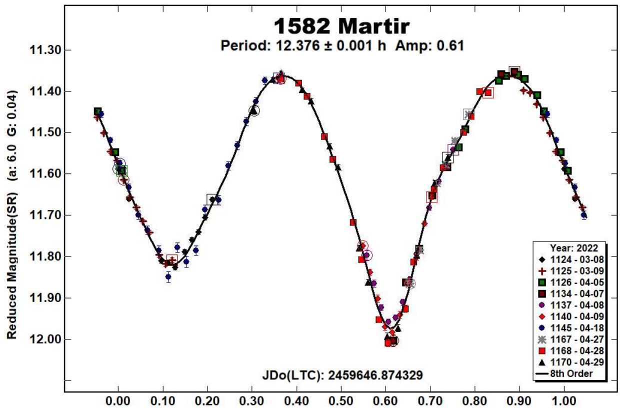

Our lightcurve coverage is complete despite the period's proximity to ½ sidereal day. The resulting period spectrum is reassuring, with signals only at multiples of half our proposed period. It does not support periods near 9.8 h (an alias of our solution by ½ period per 24 h) or near 15.6 h.

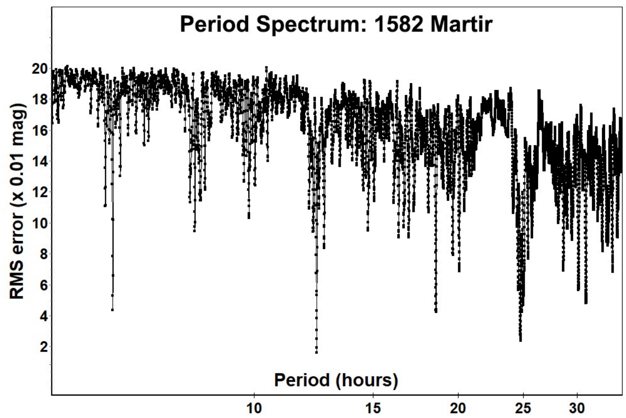

1585 Union. Of the rotation period reports for this relatively bright outer main-belt asteroid (9.38 h, Binzel, 1987; 24 h, Behrend, 2004web; 12.798 h, Polakis, 2019; 12.7993 h, Ďurech et al., 2020; 12.7988 h, Pál et al., 2020) we confirm the more recent of these with our estimate of 12.800 ± 0.001 h. The lightcurve shape is clearly bimodal. Our Fourier fit RMS error is 11 mmag, and our best estimate of G is 0.17.

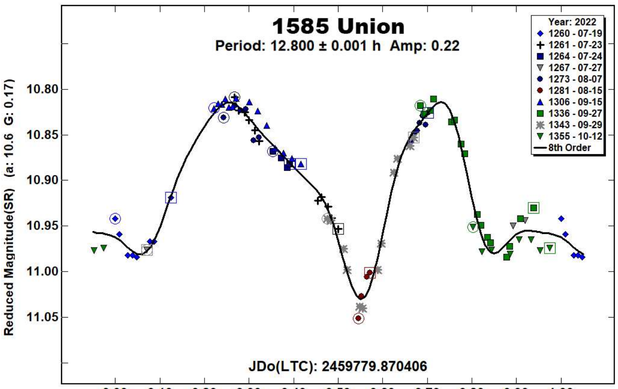

1605 Milankovitch. Our new rotation period estimate for this outer main-belt asteroid agrees with two published periods (11.60 h, Cooney, 2005; 11.63 h, Behrend, 2006web) but differs from two others (11.111 h, Carreño et al., 2020; 5.80104 h, Pál et al., 2020).

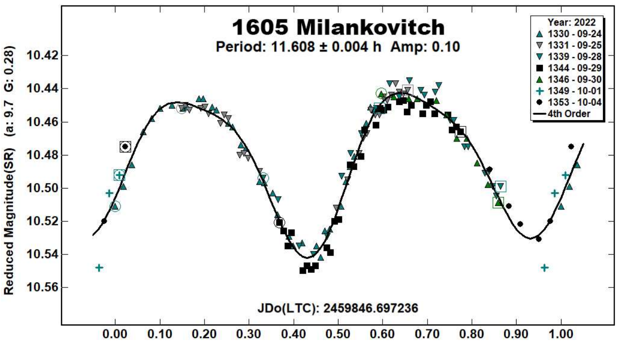

The period spectrum strongly disfavors other period candidates that are not multiples of our estimate. The published estimate of 11.111 h cannot readily be explained as an alias of our result.

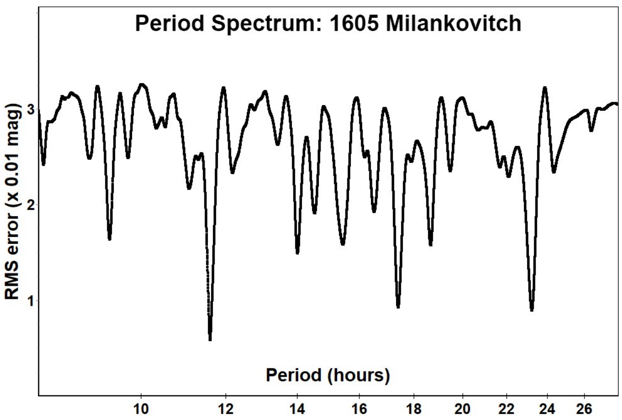

At the aspect from which our observations were taken, the lightcurve is very probably bimodal; in particular, the minima do not quite coincide in magnitude.

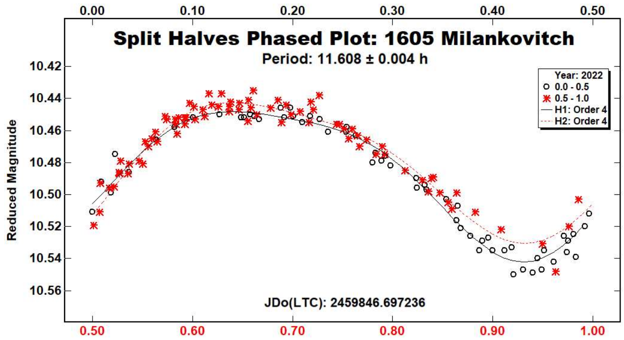

1724 Vladimir. For this outer main-belt asteroid, we confirm previous period reports, all with LCDB uncertainty codes of 2 (12.57 h, Benishek, 2011web; 12.582 h, Benishek, 2015; 12.574 h and 12.557 h, Waszczak et al., 2015; 12.56792 h, Ďurech et al., 2020), with our determination of 12.569 ± 0.002 h. Our Fourier fit RMS error is 17 mmag; G value of 0.04 minimized that fit error.

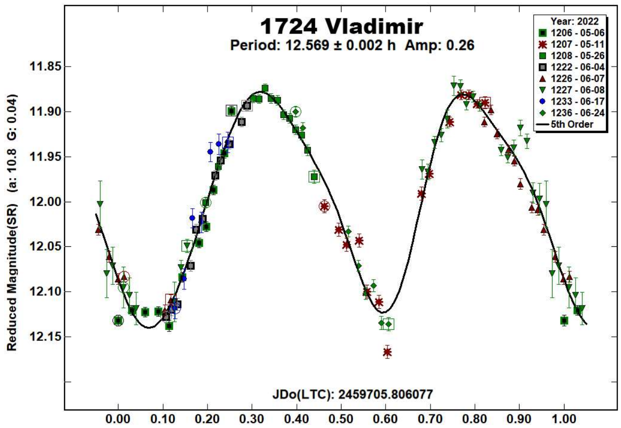

1904 Massevitch. For this outer main-belt asteroid, we confirm previous period reports (5.394 h, Bohn et al., 2015; 5.395389 h, Ďurech et al., 2019) with our finding of 5.3961 ± 0.0006 h. RMS fit error is 12 mmag; G value of 0.30 optimized the fit.

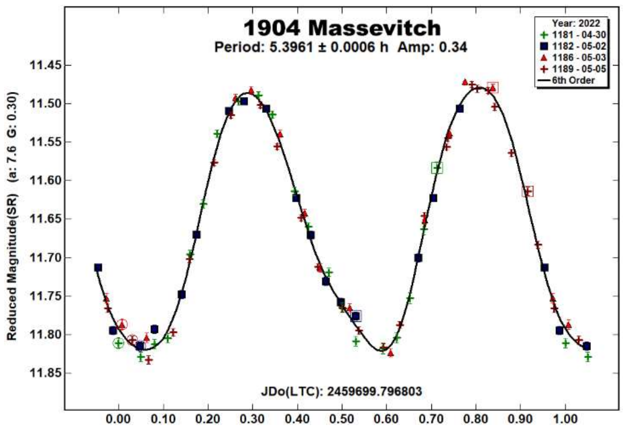

The period spectrum has secondary signals at multiples of half of our proposed period; the deepest minimum is at our proposed period.

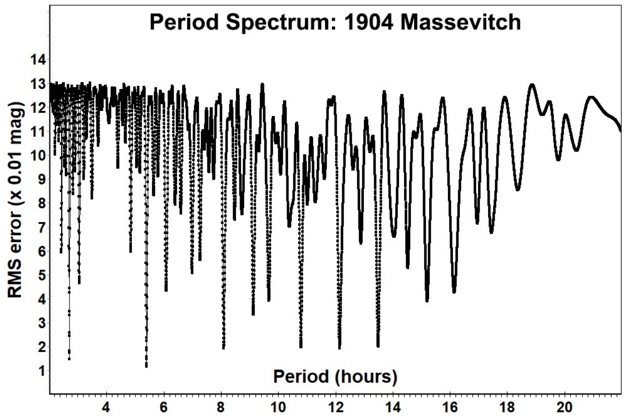

2088 Sahlia. This Flora-family asteroid has had three period reports, all differing (10.37 h, Binzel and Mulholland, 1983; 36.717 h, Erasmus et al., 2020; 58.3 h, Podlewska-Gaca et al., 2021). We generally confirm the most recent with our estimate of 59.550 ± 0.008 h. RMS error is 24 mmag; G value of 0.27 optimizes the Fourier fit.

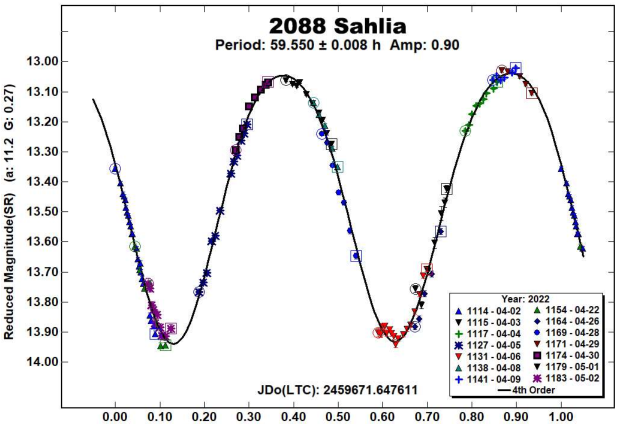

The very high lightcurve amplitude persuades us to adopt the bimodal interpretation at 59.550 h. Our period spectrum does not support previously reported periods near 10.4 h or 36.7 h (which is an alias of the present solution by exactly ¼ period per 24 h). Given the period's proximity to 60 h (2.5 days), this asteroid will benefit from longer observing sessions at apparitions of favorable latitude, of which the next will be August 2023 for the Southern Hemisphere and January 2025 for the Northern Hemisphere.

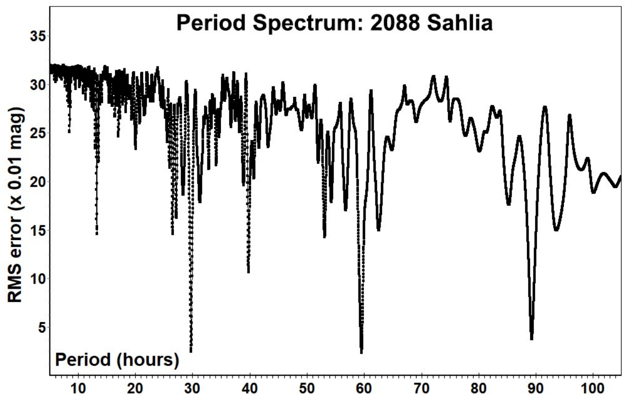

2802 Weisell. For this outer main-belt asteroid we report a period of 21.086 ± 0.003 h, in agreement with three previous reports (21.11 h, Behrend, 2006web; 21.078 h, Behrend, 2011web; 21.0966 h, Ďurech et al., 2019) but differing from two others (14.683 h, Brinsfield, 2011; 37.705 h, Hanuš et al., 2016).

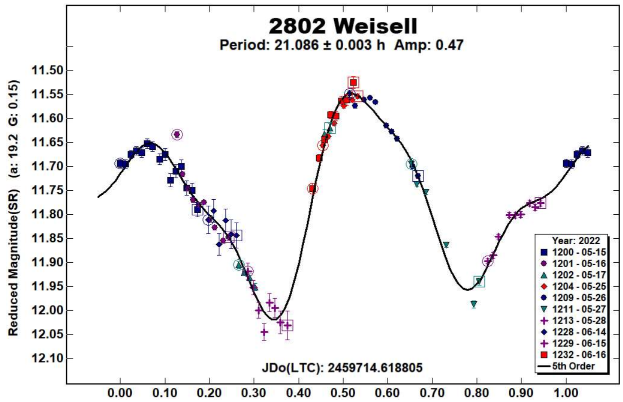

The period spectrum's strongest signal is at the proposed period, and the next-largest is at three-halves the proposed period. It does not support periods near 14.68 h or 37.7 h, both in fact being aliases of our solution by ½ period per 24 h.

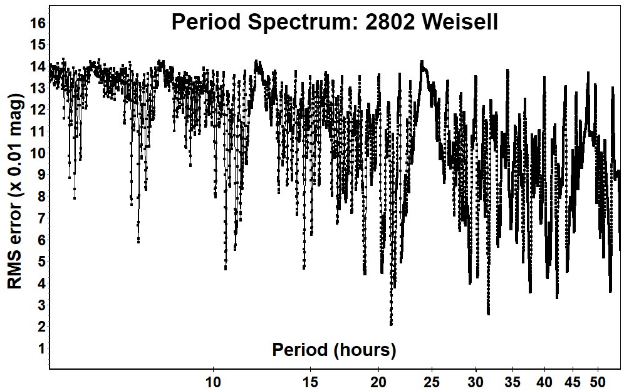

3431 Nakano. All known previous rotation period reports (8.90 h, Warner, 2003; 9.2 h, Warner, 2011; 9.0863 h, Brincat, 2017web; 9.0563 h, Brincat and Galdies, 2018; 9.05427 h, Ďurech et al., 2020) for this outer main-belt asteroid are near 9 hours, and our period estimate of 9.056 ± 0.002 h confirms them. The lightcurve shape is clearly bimodal. Fourier fit RMS error is 10 mmag, and our best estimate of G is 0.11.

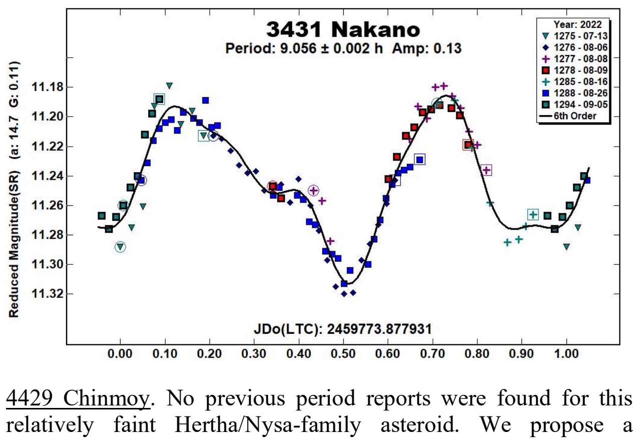

4429 Chinmoy. No previous period reports were found for this relatively faint Hertha/Nysa-family asteroid. We propose a bimodal-basis rotation period of 731.7 ± 5.0 h, based on observations over 15 nights. The observation campaign covered only 40 calendar days, or about 1.3 rotation periods, but the large apparent amplitude helped us discern the lightcurve shape early on. The Fourier fit RMS error is 35 mmag; we could not distinguish the G value from MPC's default value of 0.15.

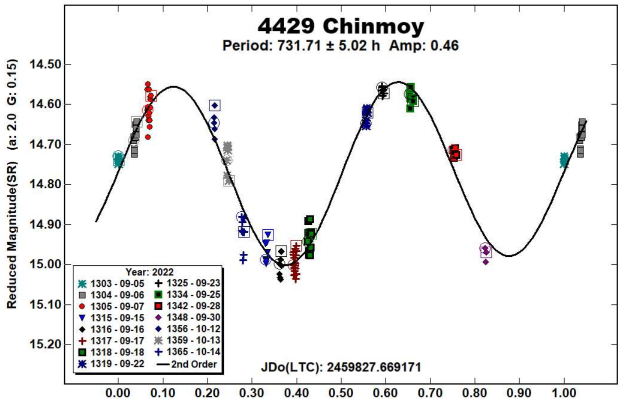

The minimum in our period spectrum actually falls at 366 h, that is, at half our proposed period estimate, but the lightcurve's large amplitude persuades us to adopt the bimodal value instead. In any case, periods shorter than about 300 h appear to be ruled out.

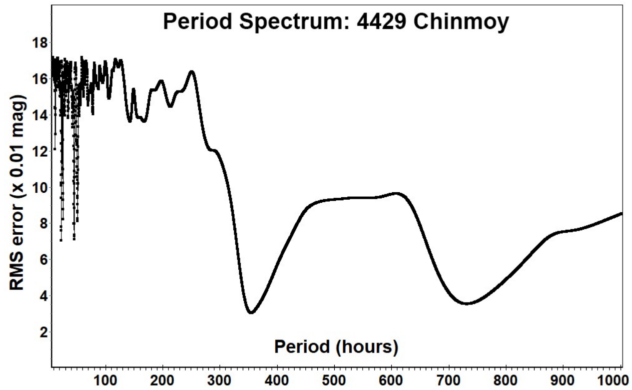

4901 O Briain. This Levin-family asteroid has no known rotation period reports. Our estimate of 1.3250 ± 0.0005 h on a monomodal basis would classify this asteroid squarely as a fast rotator, but interpreting the lightcurve as bimodal would render it a more normal case. Neither the split-halves plot nor the amplitude of 0.08 magnitudes helps to decide between monomodal and bimodal possibilities and thus the true, physical rotation rate. Our Fourier fit RMS error is 16 mmag, and our G estimate is 0.29.

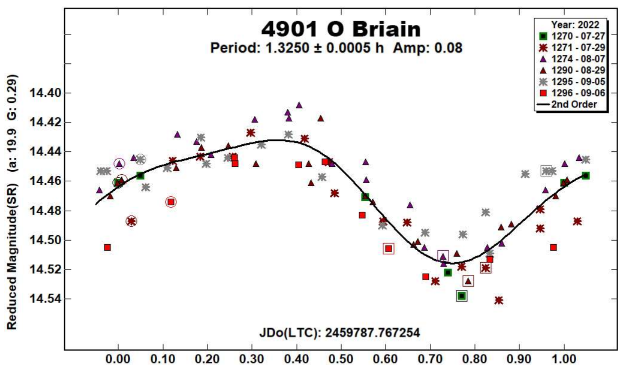

The period spectrum strongly supports our proposed period estimate, but it does not help in choosing between monomodal and bimodal lightcurve interpretations. The possibility of (4901) O Briain's being a fast rotator makes it an attractive candidate for future observation campaigns.

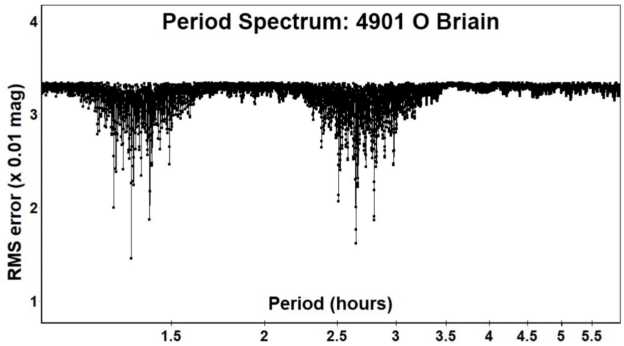

12919 Tomjohnson. This inner main-belt asteroid has no known rotation period reports. Despite the unfavorable declination for our observing site which served to limit duration of our observing sessions, we obtained an estimated period of 8.149 ± 0.001 h. The relatively large lightcurve amplitude lends confidence to the bimodal interpretation as suggested by the differing brightnesses of alternating minima. Fourier fit RMS error is 28 mmag, and our G estimate is 0.12.

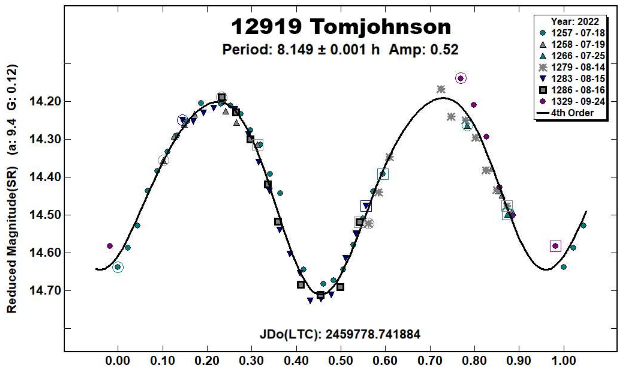

The four major signals within the period spectrum comprise a series of 1, 1.5, 2, and 2.5 times our proposed period. Despite the period's proximity to 8 hours (one-third day), other aliases have been suppressed by the use of data from seven nights variously spaced.

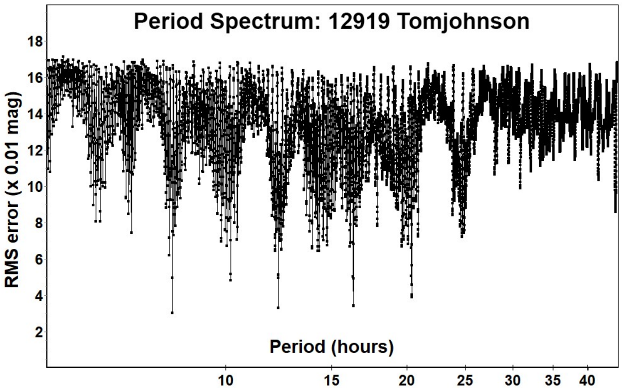

Acknowledgements

The author thanks authors of and contributors to the ATLAS paper (Tonry et al., 2018) for providing openly and without cost the ATLAS refcat2 catalog release. This current work also makes extensive use of the python language interpreter and of several supporting packages (notably: astropy, ccdproc, ephem, matplotlib, pandas, photutils, requests, and statsmodels), all made available openly and without cost.

References

Aznar Macías, A.; Carreno Garcerain, A.; Arce Masego, E.; Brines Rodriques, P.; Lozano de Haro, J.; Fornas Silva, A.; Fornas Silva, G.; Mas Martinez, V.; Rodrigo Chiner, O.; Herrero Porta, D. (2016). "Twenty-one Asteroid Lightcurves at Group Observadores de Asteroides (OBAS): Late 2015 to Early 2016." *Minor Planet Bull*. **43**, 257-263.

Behrend, R. (2004web, 2005web, 2006web, 2008web, 2009web, 2011web, 2012web, 2018web). Observatoire de Genève web site. *http://obswww.unige.ch/~behrend/page_cou.html*

Benishek, V. (2011web). *http://beoastrophot.freehostia.com* Web page not accessible July 2022; data retrieved from LCDB entry.

Benishek, V. (2015). "Rotation Period Determinations for 1724 Vladimir, 3965 Konopleva, and 9222 Chubey." *Minor Planet Bull.* **42**, 143-144.

Binzel, R.P.; Mulholland, J.D. (1983). "A photoelectric lightcurve survey of small main belt asteroids." *Icarus* **56**, 519-533.

Binzel, R.P. (1987). "A photoelectric survey of 130 asteroids." *Icarus* **72**, 135-208.

Bohn, L; Hibbler, B.; Stein, G.; Ditteon, R. (2015). "Asteroid Lightcurve Analysis at the Oakley Southern Sky Observatory: 2014 September." *Minor Planet Bull.* **42**, 89-90.

Bonamico, R.; van Belle, G. (2021). "Determining the Rotational Period of Main-Belt Asteroid 282 Clorinde." *Minor Planet Bull*. **48**, 210.

Brincat (2017web). As retrieved October 2022 from the Lightcurve Database (LCDB), reference to web page not available.

Brincat, S.M.; Galdies, C. (2018). "Photometric Observations of Main-Belt Asteroids 1968 Mehltretter, 2681 Ostrovskij & 3431 Nakano." *Minor Planet Bull*. **45**, 244-245.

Brinsfield, J.W. (2011). "Asteroid Lightcurve Analysis at the Via Capote Observatory: 1st Quarter 2011." *Minor Planet Bull.* **38**, 154-155.

Carbo, L.; Green, D.; Kragh, K.; Krotz, J.; Meiers, A.; Patino, B.; Pligge, Z.; Shaffer, N.; Ditteon, R. (2009). "Asteroid Lightcurve Analysis at the Oakley Southern Sky Observatory: 2008 October thru 2009 March." *Minor Planet Bull.* **36**, 152-157.

Carreño, A.; Fornas, G.; Arce, E.; Mas, V. (2020). "Twelve Main Belt Asteroids, One Near Earth and One Potentially Hazardous Asteroid Lightcurves at Asteroids Observers (OBAS) - MPPD: 2017 May - 2019 Jan." *Minor Planet Bull.* **47**, 7-10.

Colazo, L.C.; Fornari, C.; Santucho, M.; Mottino, A.; Colazo, C.; Melia, R.; Suarez, N.; Vasconi, N.; Arias, D.; Stechina, A.; Scotta, D.; García, J.; Pittari, C.; Ferrero, G. (2020). "Asteroid Photometry and Lightcurve Analysis at GORA's Observatories - Part II." *Minor Planet Bull*. **47**, 337-339.

Cooney, W.R., Jr. (2005). "Lightcurve Results for Minor Planets 228 Agathe, 297 Caecillia, 744 Aguntina, 1062 Ljuba, 1605 Milankovitch, and 3125 Hay." *Minor Planet Bull*. **32**, 15-16.

Dose, E. (2020). "A New Photometric Workflow and Lightcurves of Fifteen Asteroids." *Minor Planet Bull*. **47**, 324-330.

Dose, E. (2021a). "Lightcurves of Nineteen Asteroids." *Minor Planet Bull*. **48**, 69-76.

Dose, E. (2021b). "Lightcurves of Eighteen Asteroids." *Minor Planet Bull.* **48**, 125-132.

Dose, E.V. (2021c). "Lightcurves of Fourteen Asteroids." *Minor Planet Bull.* **48**, 228-233.

Ďurech, J.; Hanuš, J.; Alí-Lagoa, V. (2018). "Asteroid models reconstructed from the Lowell Photometric Database and WISE data." *Astron. Astrophys.* **617**, A57.

Ďurech, J.; Hanuš, J.; Vančo, R. (2019). "Inversion of asteroid photometry from *Gaia* DR2 and the Lowell Observatory photometric database." *Astron. Astrophys.* **631**, A2.

Ďurech, J.; Tonry, J.; Erasmus, N.; Denneau, L.; Heinze, A.N.; Flewelling, H.; Vančo, R. (2020). "Asteroid models reconstructed from ATLAS photometry." *Astron. Astrophys.* **643**, A59.

Erasmus, N.; Navarro-Meza, S.; McNeill, A.; Trilling, D.E.; Sickafoose, A.A.; Denneau, L.; Flewelling, H.; Heinze, A.; Tonry, J.L. (2020). "Investigating Taxonomic Diversity within Asteroid Families through ATLAS Dual-band Photometry." *Astrophys J. Suppl. Series* **247**, 13.

Hanuš, J.; Ďurech, J.; Broz, M.; Marciniak, A.; Warner, B.D. and 115 colleagues (2013). "Asteroids' physical models from combined dense and sparse photometry and scaling of the YORP effect by the observed obliquity distribution." *Astron. Astrophys*. **551**, A67.

Hanuš, J.; Ďurech, J.; Oszkiewicz, D.A.; Behrend, R.; Carry, B. and 164 colleagues (2016). "New and updated convex shape models of asteroids based on optical data from a large collaboration network." *Astron. Astrophys.* **586**, A108.

Harris, A.W.; Young, J.W.; Scaltriti, F.; Zappalà, V. (1984). "Lightcurves and phase relations of the asteroids 82 Alkmene and 444 Gyptis." *Icarus* **57**, 251-258.

Harris, A.W.; Pravec, P.; Galad, A.; Skiff, B.A.; Warner, B.D.; Vilagi, J.; Gajdos, S.; Carbognani, A.; Hornoch, K.; Kusnirak, P.; Cooney, W.R.; Gross, J.; Terrell, D.; Higgins, D.; Bowell, E.; Koehn, B.W. (2014). "On the maximum amplitude of harmonics on an asteroid lightcurve." *Icarus* **235**, 55-59.

McNeill, A.; Mommert, M.; Trilling, D.E.; Llama, J.; Skiff, B. (2019). "Asteroid Photometry from the Transiting Exoplanet Survey Satellite: A Pilot Study." *Astrophys J. Suppl. Series* **245**, 29.

Pál, A.; Szakáts, R.; Kiss, C.; Bódi, A.; Bognár, Z.; Kalup, C.; Kiss, L.L.; Marton, G.; Molnár, L.; Plachy, E.; Sárneczky, K.; Szabó, G.M.; Szabó, R. (2020). "Solar System Objects Observed with TESS - First Data Release: Bright Main-belt and Trojan Asteroids from the Southern Survey." *Ap. J.* **247**, A26.

Pilcher, F. (2022). "Lightcurves and Rotation Periods of 233 Asterope, 240 Vanadis, 275 Sapientia, 282 Clorinde, 414 Liriope, and 542 Susanna." *Minor Planet Bull*. **49**, 346-349.

Podlewska-Gaca, E.; Poleski, R.; Bartczak, P.; McDonald, I.; Pál, A. (2021). "Determination of Rotation Periods for a Large Sample of Asteroids from the K2 Campaign 9." *Astrophys. J. Suppl. Series* **255**, 4.

Polakis, T. (2018a). "Lightcurve Analysis for Eleven Main-Belt Asteroids." *Minor Planet Bull*. **45**, 199-203.

Polakis, T. (2018b). "Lightcurve Analysis for Fourteen Main-Belt Minor Planets." *Minor Planet Bull*. **45**, 347-352.

Polakis, T. (2019). "Lightcurves of Twelve Main-Belt Minor Planets." *Minor Planet Bull*. **46**, 287-292.

Polakis, T. (2022). "Lightcurves for Sixteen Minor Planets." *Minor Planet Bull*. **49**, 298-303.

Stephens, R.D. (2002). "Photometry of 866 Fatme, 894 Erda, 1108 Demeter, and 3443 Letsungdao." *Minor Planet Bull*. **29**, 2-3.

Stephens, R.D.; Warner, B.D. (2021). "Main-Belt Asteroids Observed from CS3: 2020 July to September." *Minor Planet Bull.* **48**, 56-69.

Tonry, J.L.; Denneau, L.; Flewelling, H.; Heinze, A.N.; Onken, C.A.; Smartt, S.J.; Stalder, B.; Weiland, H.J.; Wolf, C. (2018). "The ATLAS All-Sky Stellar Reference Catalog." *Astrophys. J.* **867**, A105.

Warner, B.D. (2000). "Lightcurve Parameters for 1582 Martir." *Minor Planet Bull.* **27**, 53-54.

Warner, B.D. (2003). "Lightcurve Analysis of Asteroids 331, 795, 886, 1266, 2023, 3285, and 3431." *Minor Planet Bull.* **30**, 61-64.

Warner, B.D. (2006). "Asteroid Lightcurve Analysis at the Palmer Divide Observatory - Late 2005 and Early 2006." *Minor Planet Bull.* **33**, 58-62.

Warner, B.D.; Harris, A.W.; Pravec, P. (2009). "The asteroid lightcurve database." *Icarus* **202**, 134-146.
https://minplanobs.org/MPInfo/php/lcdb.php

Warner, B.D. (2010). "Upon Further Review: II. An Examination of Previous Lightcurve Analysis from the Palmer Divide Observatory." *Minor Planet Bull.* **37**, 150-151.

Warner, B.D. (2011). "Upon Further Review: III. An Examination of Previous Lightcurve Analysis from the Palmer Divide Observatory." *Minor Planet Bull.* **38**, 21-23.

Warner, B.D. (2021). *MPO Canopus* Software, version 10.8.4.11. BDW Publishing. *http://www.bdwpublishing.com*

Waszczak, A.; Chang, C.-K.; Ofek, E.O.; Laher, R.; Masci, F.; Levitan, D.; Surace, J.; Cheng, Y.-C.; Ip, W.-H.; Kinoshita, D.; Helou, G.; Prince, T.A.; Kulkarni, S. (2015). "Asteroid Light Curves from the Palomar Transient Factory Survey: Rotation Periods and Phase Functions from Sparse Photometry." *Astron. J.* **150**, A75.